Report

Cell Reports

Prefrontal and Auditory Input to Intercalated Neurons of the Amygdala

Graphical Abstract

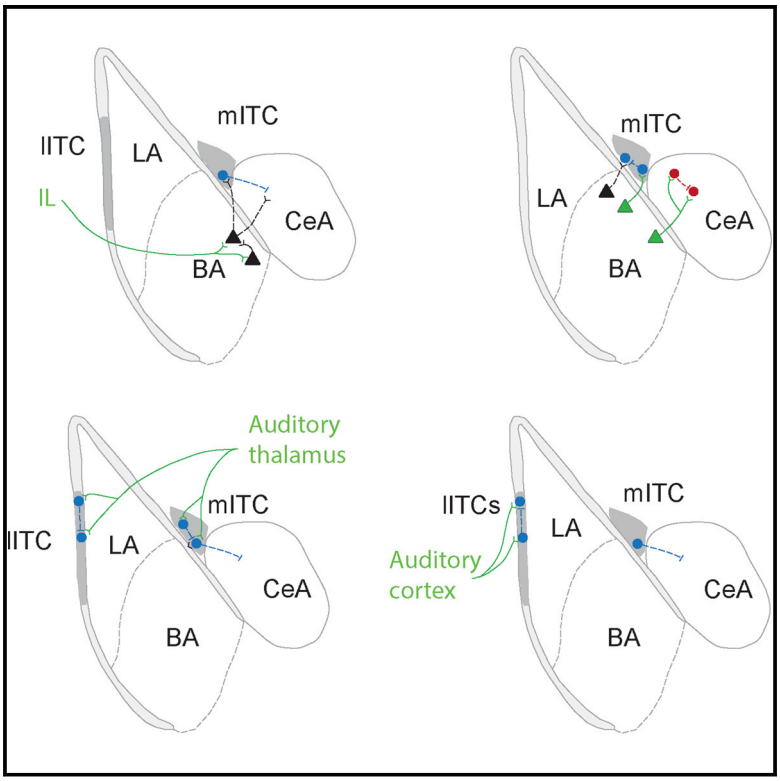

Authors

Cornelia Strobel, Roger Marek, ..., Robert K.P. Sullivan, Pankaj Sah

Correspondence

pankaj.sah@uq.edu.au

In Brief

Strobel et al. show that lateral and medial intercalated (ITC) neurons receive auditory inputs. Infralimbic prefrontal (IL) inputs do not directly innervate medial ITCs but connect via the basal amygdala (BA). These findings suggest that ITC neurons may be involved in fear learning but that the role of ILs in extinction is likely mediated via the BLA.

Highlights

- Lateral intercalated neurons receive auditory input from both cortex and thalamus
- Auditory input to medial ITC neurons is strong from thalamus but weak from cortex
- Prefrontal IL inputs innervate BLA principal neurons but not medial ITC neurons
- Excitation of medial ITC neurons from the IL is disynaptic via the basolateral amygdala

Strobel et al., 2015, Cell Reports *10*, 1435–1442
March 10, 2015
http://dx.doi.org/10.1016/j.celrep.2015.02.008

CellPress

Cell Reports
Report

Prefrontal and Auditory Input to Intercalated Neurons of the Amygdala

Cornelia Strobel,[1,2] Roger Marek,[1,2] Helen M. Gooch,[1,2] Robert K.P. Sullivan,[1] and Pankaj Sah[1,*]
[1]The Queensland Brain Institute, The University of Queensland, Brisbane, QLD 4072, Australia
[2]Co-first author
*Correspondence: pankaj.sah@uq.edu.au
http://dx.doi.org/10.1016/j.celrep.2015.02.008

SUMMARY

The basolateral amygdala (BLA) and prefrontal cortex (PFC) are partners in fear learning and extinction. Intercalated (ITC) cells are inhibitory neurons that surround the BLA. Lateral ITC (lITC) neurons provide feed-forward inhibition to BLA principal neurons, whereas medial ITC (mITC) neurons form an inhibitory interface between the BLA and central amygdala (CeA). Notably, infralimbic prefrontal (IL) input to mITC neurons is thought to play a key role in fear extinction. Here, using targeted optogenetic stimulation, we show that lITC neurons receive auditory input from cortical and thalamic regions. IL inputs innervate principal neurons in the BLA but not mITC neurons. These results suggest that (1) these neurons may play a more central role in fear learning as both lITCs and mITCs receive auditory input and that (2) mITC neurons cannot be driven directly by the IL, and their role in fear extinction is likely mediated via the BLA.

INTRODUCTION

Fear conditioning and extinction are behavioral paradigms widely used to study learning and memory formation in the mammalian CNS. In fear conditioning, a neutral stimulus, such as a tone (the conditioned stimulus, CS), is temporally paired with an aversive stimulus, typically, a footshock. As a result, subjects now respond to the previously neutral stimulus with a fear response, which represents the recall of an associative fear memory. However, subsequent unpaired presentations of the CS leads to a reduction of the fear response, a process known as extinction (Delamater, 2004). The neural circuits that underpin fear conditioning and extinction have been extensively studied, and it is well established that the amygdala and prefrontal cortex are two key players (Duvarci and Pare, 2014; Marek et al., 2013; Maren, 2001; Pape and Pare, 2010). During auditory fear conditioning, tone information reaches the amygdala via direct projections from the auditory thalamus (AT) and auditory cortex (AC), predominantly synapsing within the basolateral amygdala (BLA) (LeDoux et al., 1991; Romanski et al., 1993; Romanski and LeDoux, 1993; Sah et al., 2003). Sensory information is processed within the amygdala, and projections from the central amygdala (CeA), the main output region of the amygdala, trigger the physiological responses associated with the fear response (Davis and Whalen, 2001; Maren, 2001).

The BLA is a cortical-like structure, and glutamatergic pyramidal neurons form the major population of neurons within it (~80%) (McDonald, 1982; Sah et al., 2003). A heterogeneous population of GABAergic interneurons constitutes a smaller population of cells (~20%), providing both feed-forward and feedback inhibition within the amygdala (Ehrlich et al., 2009; McDonald, 1985; Spampanato et al., 2011). Apart from local GABAergic interneurons within the BLA, clusters of small GABAergic cells, the intercalated (ITC) cell masses, also surround the BLA (Millhouse, 1986; Pinard et al., 2012). ITC cells are divided into the lateral ITC (lITC) and medial ITC (mITC) clusters, located within the external and intermediate capsules of the amygdala, respectively. Of these, lITC neurons provide feed-forward inhibition for cortical afferents to BLA pyramidal neurons (Marowsky et al., 2005; Morozov et al., 2011), while mITC neurons are thought to form an inhibitory interface between the input (BLA) and output (CeA) nuclei of the amygdala (Palomares-Castillo et al., 2012; Pare and Duvarci, 2012; Paré and Smith, 1993).

It is generally accepted that fear learning engages the BLA and results from plasticity of sensory inputs to BLA pyramidal neurons (Miserendino et al., 1990; Pape and Pare, 2010; Quirk et al., 1995; Sah et al., 2003). This plasticity is, at least in part, regulated by the action of local inhibitory microcircuits in the BLA (Ehrlich et al., 2009; Wolff et al., 2014). Following learning, expression of learned fear is driven by afferents from the prelimbic medial prefrontal cortex to the BLA (Corcoran and Quirk, 2007; Sotres-Bayon et al., 2012). While extinction also engages the BLA (Falls et al., 1992; Herry et al., 2006; Laurent and Westbrook, 2008), it is thought to be gated by infralimbic prefrontal cortex (IL) activity (Milad and Quirk, 2002; Sierra-Mercado et al., 2011; Sotres-Bayon et al., 2012). Afferents from the IL are proposed to drive mITC neurons, resulting in feed-forward inhibition of the CeA thus inhibiting output from the amygdala (Amir et al., 2011; Berretta et al., 2005; Likhtik et al., 2005; Likhtik et al., 2008).

While the neural circuits within the BLA, CeA, and their afferents are reasonably well understood (Pape and Pare, 2010; Sah et al., 2003), little is known about the sources and nature of connectivity of ITC neurons. However, a recent tract-tracing study has suggested that IL inputs to the amygdala may not directly innervate mITC neurons, thus questioning the current circuit model (Pinard et al., 2012). Here, using targeted

expression of channelrhodopsin in the AC, AT, and IL, we characterize the afferent innervation of lITC and mITC neurons. These results show that lITC neurons receive auditory input from both cortical and thalamic regions. The mITC neurons receive input from the BLA but also receive strong input from the AT. However, mITC neurons are not directly innervated by afferents from the IL.

RESULTS

To study specific afferents to the amygdala, we performed targeted injections of adeno-associated virus (AAV) to selectively express the light-gated Channelrhodopsin2-yellow fluorescent protein (ChR2-YFP) in the IL, the AC, or the AT in GAD67-EGFP transgenic mice (Tamamaki et al., 2003) (Figure S1). First, we tested inputs from the IL to the amygdala. In agreement with previous anterograde tracing studies (McDonald, 1998; Vertes, 2004), transduction of YFP-tagged ChR2 in IL neurons resulted in strong afferent labeling in the basal amygdala (BA; Figure S1A3). Optical stimulation of IL afferents to the BLA (Cho et al., 2013; Hübner et al., 2014) evoked large and reliable inputs in BA pyramidal neurons (n = 9/9; Figure 1D1). Mean excitatory postsynaptic currents (EPSCs) and excitatory postsynaptic potentials (EPSPs) in pyramidal neurons located ventrally in the BA (vBA) had amplitudes of −74 ± 12 pA (holding potential, V_h, −60 mV) and 13.0 ± 0.6 mV, respectively. Evoked synaptic inputs were time locked to the light stimulus with small synaptic jitter (0.37 ± 0.07 ms) and no failures, which is consistent with a monosynaptic connection. As compared to the vBA, fewer IL terminals are apparent in more dorsal BA (dBA), neighboring the lateral amygdala (Figure S1A3). Recordings from pyramidal neurons of this dBA region revealed that optical stimulation of IL afferents evoked a significantly smaller input (mean EPSC amplitude, −16 ± 5 pA, V_h, −60 mV, n = 4/5; one-way ANOVA, $F(2, 13) = 19.1$, $p < 0.01$) compared with vBA cells, and exhibited much larger synaptic jitter (0.71 ± 0.04 ms), suggesting a polysynaptic input (Figures 1F and 1G).

ITC neurons were identified as the characteristic clusters of EGFP-expressing cells located along the lateral and medial borders of the BLA (Figures 1B2 and 1B3). Neurons in these clusters had electrophysiological properties characteristic of ITC neurons (Figures 1C2 and 1C3) (Busti et al., 2011) and expressed μ-opioid receptors (Figure S2E), confirming their identity (Jacobsen et al., 2006). As described previously (Mcdonald et al., 1996; Pinard et al., 2012; Pinto and Sesack, 2008), YFP-expressing fibers labeling afferents from the IL could be seen coursing through the mITC, but not the lITC (Figures S2C and S2D). Optical stimulation of IL afferents to ITC neurons revealed that neither lITC nor mITC received direct input from the IL (lITC, n = 4; mITC, n = 19; Figures 1D2, 1D3, and 1F). In three mITC cells, activation of IL afferents did evoke a small synaptic current (mean amplitude: EPSC, −14 ± 3 pA; EPSP, 1.5 ± 1.2 mV) that had a large onset jitter (0.8 ± 0.11 ms; Figures 1D3, 1F, and 1G) and a high failure rate (28% ± 6%), consistent with a polysynaptic input.

Electrical stimulation in the BA in acute brain slices has shown that neurons in the mITC receive excitatory input from the BA (Amano et al., 2010; Royer et al., 1999). We directly tested if pyramidal neurons in the BA project to mITC neurons by injecting AAV-ChR2 into the BLA (Figure 2A). Whole-cell recordings from YFP-positive pyramidal neurons in the BA revealed that optical stimulation evokes an inward current throughout the duration of light illumination, consistent with membrane-bound ChR2 expression (Figure 2B), and drives local neurons to threshold in response to short light pulses (5 ms, n = 2/3; Figure 2E). Recordings from mITC neurons evoked single, time-locked synaptic responses (mean EPSC amplitude, −32 ± 13 pA, n = 6; Figures 2C and 2F), with no prolonged inward current. Evoked synaptic currents showed low response jitter (0.54 ± 0.07 ms) and no failures, consistent with monosynaptic input from BA to mITC neurons. In one mITC neuron, disynaptic inhibitory postsynaptic currents (IPSCs) were also observed (Figure 2G), as expected from the connectivity within the mITC cluster (Royer et al., 2000). Neurons in the BLA (Lopez de Armentia and Sah, 2004) as well as mITC (Paré and Smith, 1993), project to the lateral central amygdala (CeL), and these neurons also responded to BA-ChR2 illumination with time-locked EPSCs, which were consistently followed by disynaptic IPSCs (n = 3; Figures 2D and 2G). While AAV-ChR2 injections to the BLA resulted in some transduction of the piriform cortex, this structure has very limited projections to the amygdala (Behan and Haberly, 1999). As described earlier, optical stimulation of IL terminals evoked polysynaptic responses with a larger jitter in mITC cells. As these responses were seen in slices in which suprathreshold IL responses were present in BA pyramidal neurons, these small IL-evoked inputs to mITC neurons are likely to be disynaptic, arising from excitation of BLA pyramidal neurons.

As expected, electrical stimulation in the BA (Figure 2H) evoked monosynaptic responses in mITC neurons (mean EPSC amplitude, −49 ± 4 pA, n = 6; Figure 2I). Tetanic stimulation of electrically evoked BLA inputs to some ITC neurons have been shown to undergo synaptic plasticity (Royer and Paré, 2003). Consistent with this, tetanic stimulation of BLA inputs to mITC neurons in GAD-67 EGFP mice also evoked long-term potentiation (LTP) in five of 25 cells tested (mean potentiation: 164% ± 9%; Student's t test, $p < 0.01$, compared to the baseline response, measured 40 min after electrical BLA stimulation; Figure 2J). However, the majority of cells tested (20 of 25) showed no significant change in synaptic strength, with a 2.4% ± 0.3% increase compared to baseline (Student's t test: $p > 0.05$; Figure 2J). Taken together, these results suggest that IL inputs to the amygdala do not innervate mITC neurons but can drive pyramidal neurons in the ventral BLA to threshold. Thus, stimulation of IL afferents evokes disynaptic excitation of mITC neurons via the BLA. Moreover, this BLA input to mITC neurons is capable of undergoing long-term synaptic plasticity.

mITC neurons provide feed-forward inhibition to the CeA (Duvarci and Pare, 2014) and have been proposed to play a key role in fear extinction, being driven by input from the IL (Duvarci and Pare, 2014; Likhtik et al., 2008). In contrast, lITC neurons are thought to provide cortical feed-forward inhibition to BLA pyramidal neurons (Marowsky et al., 2005). While mITC neurons are clearly involved in fear extinction (Likhtik et al., 2008), the role of lITC neurons is not known. We have shown that neither lITC nor mITC neurons receive input from the IL. Therefore, we asked whether ITC neurons receive input from other extra-amygdaloid brain regions known to be involved in auditory fear learning. The

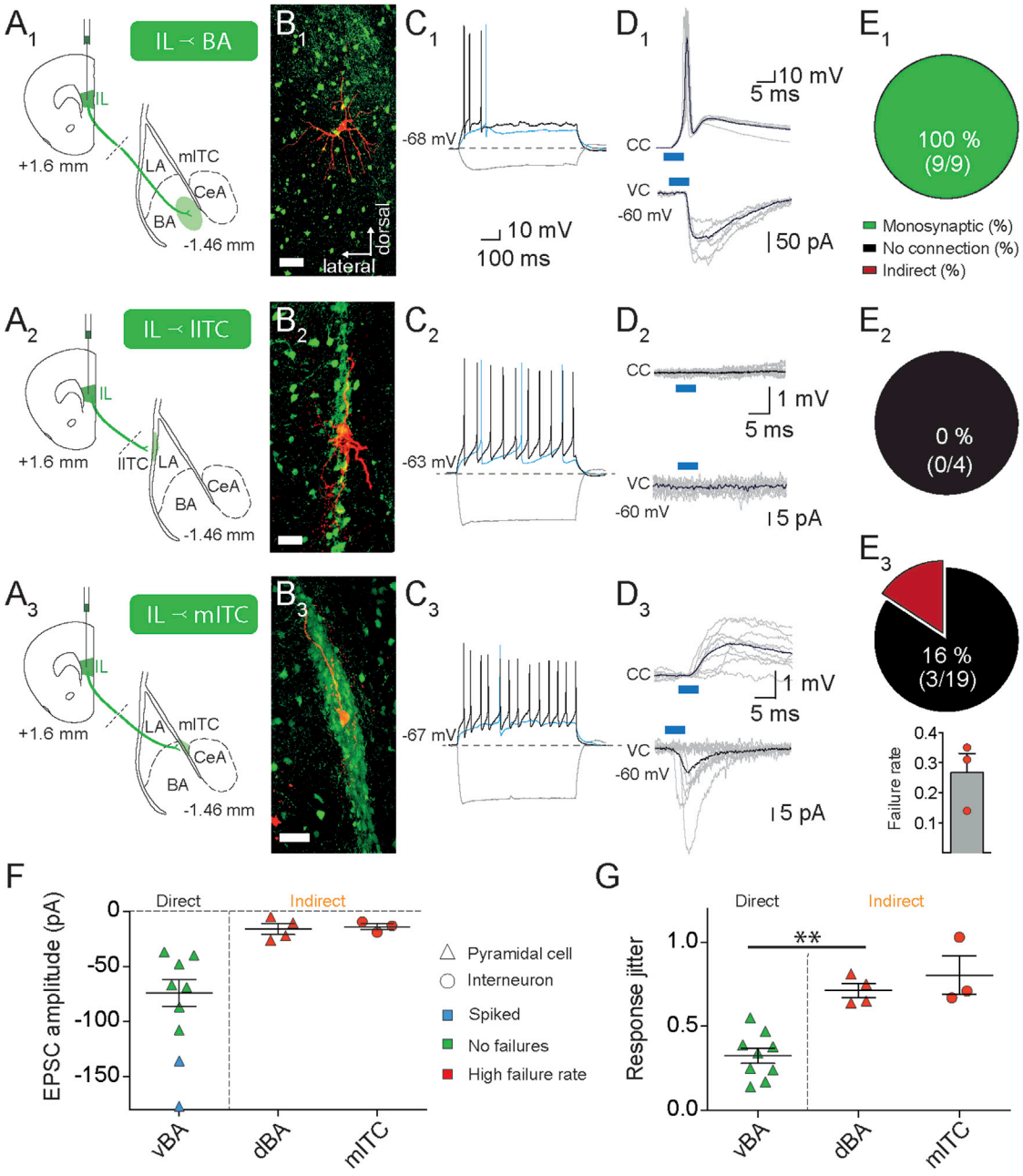

Figure 1. IL Afferents Directly Innervate BA Neurons but Not ITCs

(A_1–A_3) Schematic illustration of the injection sites for channelrhodopsin expression in the IL and recording sites for BA principal neurons (A_1), lITC (A_2), and mITC neurons (A_3). LA, lateral amygdala.

(B_1–B_3) Flattened apotome z stack images of recorded neurons: BA pyramidal neuron (B_1), lITC neuron (B_2), or mITC neuron (B_3). Neurons filled with biocytin (red) are shown in slices from GAD67-EGFP animals (green). Scale bars represent 10 μm.

(C_1–C_3) Whole-cell recordings from neurons in the BA, lITC, and mITC shown in (B). Shown is the response to current injections of −100 pA (gray), threshold (blue), and twice threshold (black). Recordings were made at the indicated resting membrane potential.

(D_1–D_3) Light-evoked (blue bars) response to stimulation of IL afferents recorded in current clamp (CC) and voltage clamp (VC; V_h, −60 mV).

(E_1–E_3) Summary pie charts showing the percentage of cells that received direct innervation (green), no innervation (black), and indirect (disynaptic) innervation (red) from the IL. The inset in (E_3) shows the failure rate, measured as the number of failures for each sampled neuron divided by the total times of light illumination, of the evoked EPSC in three mITC neurons.

(F) Summary for peak EPSC amplitudes evoked by light stimulation of IL afferents in vBA, dBA, and mITC.

(G) Plotted is the SD of EPSC onset latencies (jitter) in vBA, dBA, and mITC in response to light-evoked IL terminal stimulation. **$p < 0.01$.

Error bars indicate mean ± SEM.

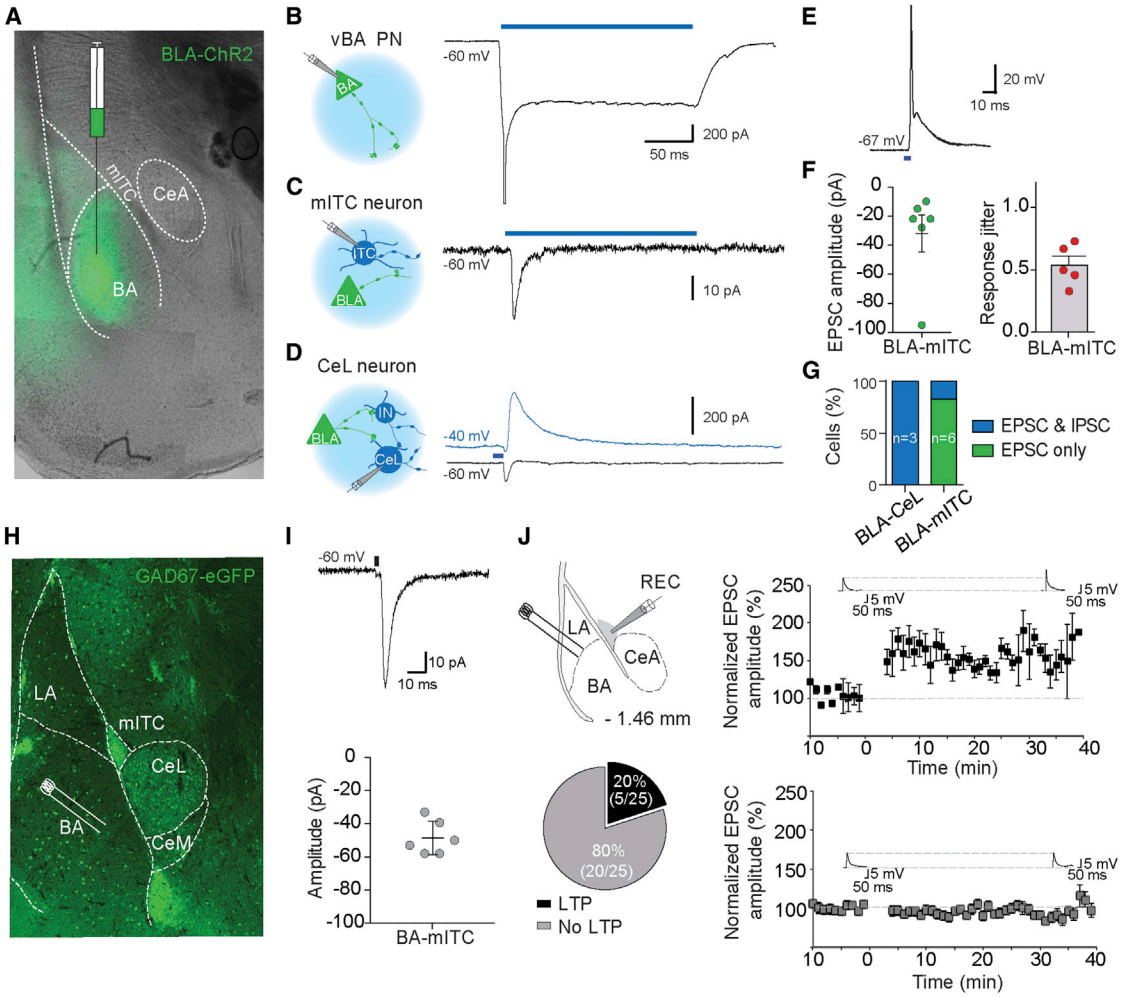

Figure 2. BLA Principal Neurons Innervate mITC Neurons

(A) Fluorescence image showing the AAV-ChR2 injection site in the BLA.

(B–D) Panels on the left show schematics illustrating stimulated inputs (green) and indicated recording sites (blue) in the BLA (B), mITC (C), and CeL (D). The traces on the right show light-evoked responses (blue bar) recorded at a V_h of −60 mV. Channelrhodopsin-transduced BA neurons showed an inward current for the duration of light stimulation (blue bar), indicating AAV-ChR2 virus transduction. mITCs were not infected, as only single, time-locked synaptic responses were observed in response to prolonged light stimulation. In CeL neurons, optical stimulation evoked EPSCs at −60 mV and IPSCs at −40 mV. PN, principal neuron.

(E) In current clamp, vBA neurons discharged action potentials in response to light stimulation.

(F) Graph on the left shows a summary plot of mean mITC EPSC amplitudes in response to optical terminal stimulation of BLA afferents. The synaptic jitter of these responses is shown on the right.

(G) Summary data showing the percentage of CeL and mITC neurons that received EPSCs and disynaptic IPSCs (blue) or EPSCs alone (green).

(H) Fluorescence image of the amygdala in a GAD67-EGFP animal with clear identification of the mITC cluster and indication of the electrical stimulation site within the BA. LA, lateral amygdala; BA, basal amygdala; mITC, medial ITC; CeL, lateral division central amygdala; CeM, medial division central amygdala.

(I) Electrical stimulation in the BA-evoked EPSCs in mITC neurons; the summary data of evoked EPSC amplitudes is shown in the histogram.

(J) BLA input to mITC neurons can undergo LTP. The schematic shows the recording and stimulation configuration. The upper panel on the right shows the response to tetanic stimulation (Experimental Procedures) of BLA input to mITC neurons. Tetanic stimulation results in LTP of the synaptic input. EPSPs recorded in the baseline (left) and 30 min following tetanic stimulation (right) are shown as insets. The lower panel shows the response to different populations of mITC neurons where tetanic stimulation had no effect on synaptic input. The pie chart shows the summary of all cells tested, with 20% of recorded neurons showing LTP. REC, recording electrode.

Error bars indicate mean ± SEM.

amygdala receives afferents from both the AT (LeDoux et al., 1984, 1991) and secondary AC (Mascagni et al., 1993; Romanski and LeDoux, 1993), and we tested inputs from the AT and AC by selectively injecting AAV-ChR2 into both regions (Figures S1B and S1C).

As expected, both AT and AC injections produced significant labeling in the lateral amygdala (Figures S1B3 and S1D3). For AT injections, YFP-expressing axons were apparent in both the lITC and mITC cell clusters (Figures S3B and S3C). For AC injections, terminal labeling was strong in the lITC cell cluster but appeared

comparatively sparse in the mITC (Figures S3D and S3E). Optical stimulation of AC afferents to lITC neurons (Figure 3A1) evoked robust synaptic responses (11 of 15; mean amplitude: EPSC, −66 ± 14 pA; EPSP, 11 ± 2 mV; Figures 3E1, 3G, and 3H). This response was time locked to the light stimulus with little jitter (0.45 ± 0.05 ms, n = 11; Figure 3I) and no failures, consistent with monosynaptic AC input to these neurons. In lITC neurons that received excitatory input from the AC, depolarization of the neuron to −40 mV revealed a disynaptic inhibitory current (n = 7/12; Figure 3J). Stimulation of AT inputs to lITC neurons (Figure 3A2) also evoked large and time-locked synaptic responses (mean amplitude: EPSC, −133 ± 44 pA; EPSP, 14 ± 3 mV, n = 7/16; jitter: 0.24 ± 0.07 ms; Figures 3E2 and 3G–3I). As with cortical input, some neurons (four of seven) also displayed a disynaptic inhibitory current. Moreover, in two neurons (two of 16), no EPSC was apparent, but a disynaptic IPSC was apparent (Figure 3J). Thus, lITC neurons receive both cortical and thalamic auditory input.

In the mITC cell cluster, most neurons (nine of 13) were monosynaptically innervated by AT inputs (Figures 3A3 and 3F3). Optical stimulation evoked time-locked synaptic responses (mean amplitude: EPSC, −72 ± 14 pA; EPSP, 10 ± 2 mV; Figures 3E$_3$, 3G, and 3H) with little onset jitter (0.30 ± 0.06 ms, n = 9; Figure 3I). Moreover, in six of nine neurons, depolarization to −40 mV revealed disynaptic inhibition (Figure 3J). Paired recordings between mITC cells have shown that these cells are synaptically coupled (Geracitano et al., 2007); thus, these disynaptic IPSCs may originate from local mITC inhibition. Optical stimulation of AC afferents to mITC neurons also evoked synaptic inputs (n = 3; Figures 3A4 and 3E4). However, this input was small (mean amplitude: EPSC, −23 ± 11 pA; EPSP, 4 ± 2 mV; Figures 2H and 3G), had a high failure rate (60% ± 3%), and had a significantly large response jitter (0.97 ± 0.08 ms; one-way ANOVA, $F(3, 26) = 13.6$; $p < 0.001$ (Figure 3I), suggesting disynaptic excitation, most likely, via the BLA. Together, these results show that mITC neurons receive strong monosynaptic input from the AT. However, input from the AC appears to be small and, likely, disynaptic.

DISCUSSION

The ITCs are clusters of inhibitory neurons that surround the BLA (Millhouse, 1986; Pinard et al., 2012) and provide inhibitory control of neurons in the BLA and CeA (Marowsky et al., 2005; Palomares-Castillo et al., 2012). lITC neurons, located within the external capsule, are thought to provide feed-forward inhibitory control for cortical input to BLA pyramidal neurons (Marowsky et al., 2005). Our results show that lITC neurons receive auditory input from both thalamic and cortical areas that is large enough to drive them to threshold. Dopamine has been shown to presynaptically depress feed-forward inhibition mediated by local interneurons in the BLA, thus facilitating plasticity of thalamic input to the BLA (Bissière et al., 2003). lITC cells are densely innervated by putative dopaminergic terminals and are inhibited by dopamine (Marowsky et al., 2005). Dopamine is released into the amygdala during stressful episodes (Inglis and Moghaddam, 1999), and dopamine receptor activity is known to affect fear learning (Guarraci et al., 1999). Our results suggest that dopaminergic input to the amygdala would result in widespread reduction of auditory feed-forward inhibition, disinhibiting pyramidal neurons in the BLA.

IL activity is required for expression of fear extinction (Milad and Quirk, 2002; Sierra-Mercado et al., 2011; Vidal-Gonzalez et al., 2006), and stimulation of the medial prefrontal cortex inhibits BLA-driven activity of the CeL (Quirk et al., 2003). The mITCs, located between the BLA and CeA, provide feed-forward inhibition between the BLA and CeA (Royer et al., 1999) and are thought to act as an inhibitory gate between these two nuclei. Neurons in the mITC cluster can be driven by the medial prefrontal cortex (Amir et al., 2011; Berretta et al., 2005), and disruption of these neurons reduces extinction (Likhtik et al., 2008). Therefore, it has been proposed that, during fear extinction, IL projections to the amygdala directly drive mITC neurons, thus inhibiting CeA output (Duvarci and Pare, 2014; Pape and Pare, 2010). Anatomical tracer studies have shown that afferents from the IL are present in the region of the mITC (Mcdonald et al., 1996; Pinard et al., 2012; Pinto and Sesack, 2008; Vertes, 2004). Using selective ChR2 expression in the IL, however, we found that neurons in the mITC cell cluster do not receive direct IL inputs. However, BA pyramidal neurons in the same slices clearly responded to IL-specific afferent stimulation, consistent with the robust density of ChR2-positive terminals in the BA. In turn, as BA neurons innervate the mITC, IL activity can drive mITC cells disynaptically via the BA. In agreement with this, activation of IL afferents did evoke small disynaptic EPSCs in some mITC neurons. Our results are in apparent contrast to recent results, where it has been suggested that mITC neurons receive large IL inputs (Cho et al., 2013). The reason for this discrepancy is not clear. It is notable, however, that, in the Cho et al. study, neurons were identified as clusters of cells in acute slices from C57Bl6 mice but were not definitively identified as being ITC neurons. In contrast, in our study, recordings were made from transgenic GAD67-EGFP mice where interneurons were identified by the EGFP expression, and ITC neurons were distinguished by μ-opioid receptor labeling (Jacobsen et al., 2006).

In summary, we have shown that both the lITC and the mITC neurons receive strong auditory input from cortical and thalamic sources. Thus, activity of these GABAergic neurons is likely to contribute to fear learning. The mITC neurons do not receive direct IL input, and we suggest that the role of these neurons in fear extinction is likely mediated by input from BA pyramidal cells. One interesting question to address in future studies is whether "extinction neurons" that are seen during fear extinction (Herry et al., 2008) may be projection neurons to the mITC.

EXPERIMENTAL PROCEDURES

GAD67-EGFP knockin mice on a C57BL/6 background were used, which allowed for the clear identification of GABAergic ITC clusters. All experimental and animal care procedures were in accordance with the Australian Code of Practice for the Care and Use of Animals for Scientific Purposes and approved by the Animal Ethics Committee for the University of Queensland. AAVs were obtained from Penn Vector Core (AAV2/5.hsynap.syn.hChR2(H134R)-GFP.W.SV40). Stereotactic viral injections were performed using standard procedures (see the Supplemental Experimental Procedures for full details).

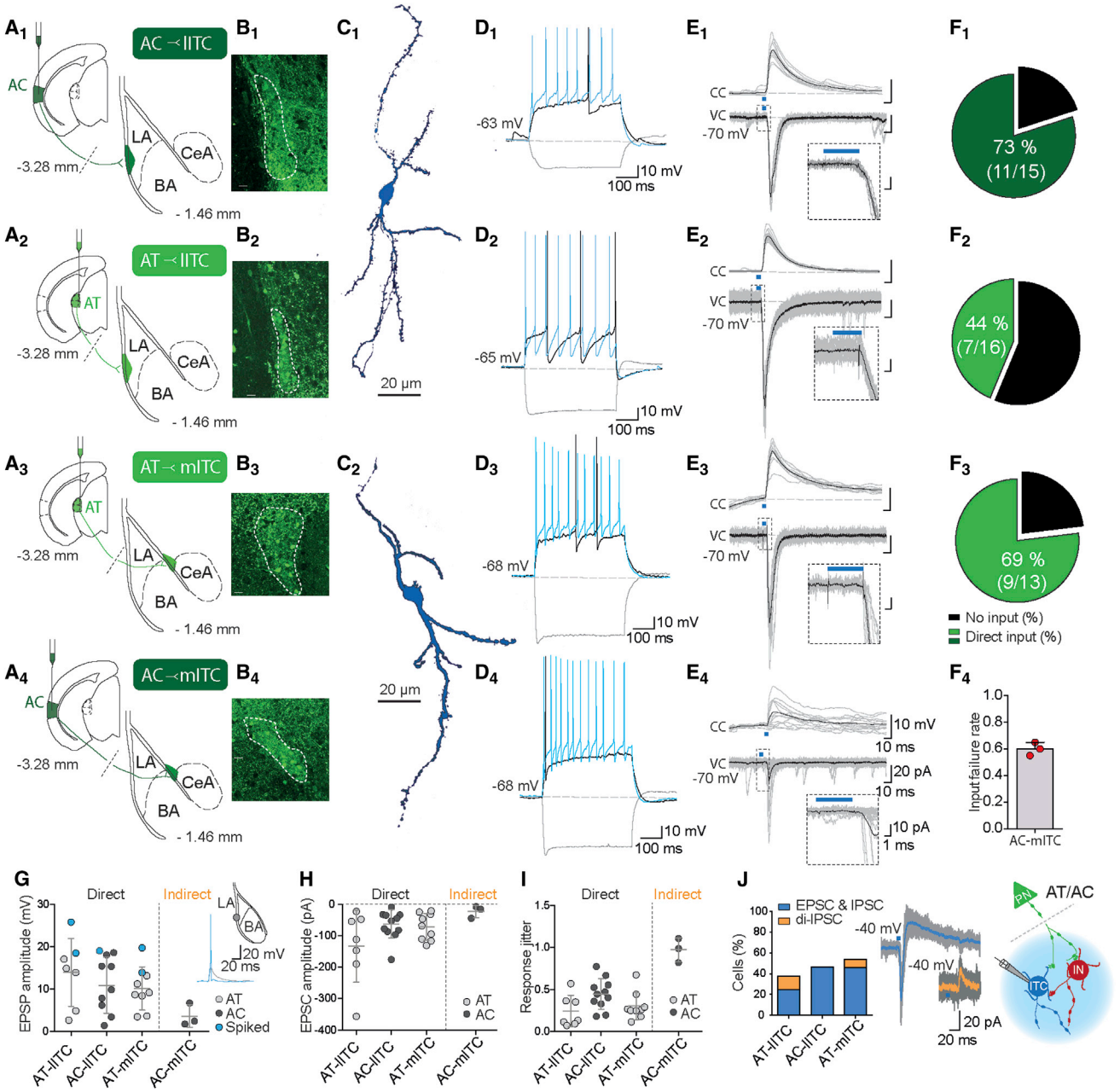

Figure 3. Auditory Afferents Innervate Both mITC and IITC Neurons

(A1–A4) Schematics illustrating injection sites in AT and AC and recording sites in IITC (A_1 and A_2) or mITC (A_3 and A_4). LA, lateral amygdala.

(B_1–B_4) Channelrhodopsin-YFP-expressing afferents (green) in the region of the IITC (B_1 and B_2) and mITC (B_3 and B_4).

(C_1 and C_2) IITC and mITC neurons were filled and subsequently immunolabeled for neurobiotin. Shown are flattened apotome z stack images of neurons recorded in the IITC (C_1) and mITC (C_2). Scale bars represent 20 µm.

(D_1–D_4) Discharge properties of IITC (D_1 and D_2) and mITC neurons (D_3 and D_4) in response to somatic current injections of −75 pA (gray), threshold (black), and twice threshold (blue). Recordings were made from resting potential as indicated.

(E_1–E_4) Light (blue bar)-evoked AT and AC responses recorded in current clamp (top) or voltage clamp (bottom; V_h, −70 mV) in neurons in the IITC (E_1 and E_2) or mITC (E_3 and E_4). The inset shows a magnified image of the traces recorded in voltage clamp to highlight onset latencies.

(F_1–F_4) Pie charts summarize the percentage of cells that received direct (green) or indirect (black) inputs from the AC (F_1) and AT (F_2 and F_3). The failure rate of three mITCs, measured as the number of failures for each sampled neuron divided by the total number of light illuminations, is shown in (F_4).

(G and H) Summary plot of EPSP (G) and EPSC (H) amplitudes in IITCs and mITCs, in response to light-evoked AT (light gray) and AC (dark gray) terminal stimulation. Direct and indirect connections are labeled and separated by the dashed line. Cells that were driven to threshold are indicated in blue.

(I) Synaptic onset jitter of light-evoked EPSCs in IITC and mITC neurons for AT (light gray) and AC (dark gray) terminal stimulation.

(legend continued on next page)

Acute brain slices were prepared and maintained at 32 ± 2°C during whole-cell recordings using standard procedures. Current and voltage-clamp recordings were made using a MultiClamp 700B amplifier (Molecular Devices). Recordings were filtered at 6 kHz and digitized at 10–20 kHz using an ITC-18 (InstruTech). Recordings were acquired and analyzed offline using Axograph X. ChR2-infected axonal projections were driven with 5-ms, 0.1-Hz, whole-field LED illumination at blue excitation wavelengths ~470 nm long (CAIRN OptoLED or CoolLED), and light-evoked photocurrents were recorded in whole-cell patch-clamp configuration. The light intensity at the specimen was 5.3 mW/mm^2. Data are expressed as mean ± SEM.

SUPPLEMENTAL INFORMATION

Supplemental Information includes Supplemental Experimental Procedures and three figures and can be found with this article online at http://dx.doi.org/10.1016/j.celrep.2015.02.008.

AUTHOR CONTRIBUTIONS

P.S. conceived the project and wrote the manuscript. C.S., R.M., and H.M.G. performed the experiments, analyzed the data, and wrote the manuscript. R.K.P.S. performed the immunohistochemistry.

ACKNOWLEDGMENTS

We thank members of the lab and Alan Woodruff for comments on the manuscript. This work was supported by grants from the Australian National Health and Medical Research Council and the Australian Research Council Centre for Integrative Brain Function (CIBF) CE140100007.

Received: November 7, 2014
Revised: January 17, 2015
Accepted: January 29, 2015
Published: March 5, 2015

REFERENCES

Amano, T., Unal, C.T., and Paré, D. (2010). Synaptic correlates of fear extinction in the amygdala. Nat. Neurosci. *13*, 489–494.

Amir, A., Amano, T., and Pare, D. (2011). Physiological identification and infralimbic responsiveness of rat intercalated amygdala neurons. J. Neurophysiol. *105*, 3054–3066.

Behan, M., and Haberly, L.B. (1999). Intrinsic and efferent connections of the endopiriform nucleus in rat. J. Comp. Neurol. *408*, 532–548.

Berretta, S., Pantazopoulos, H., Caldera, M., Pantazopoulos, P., and Paré, D. (2005). Infralimbic cortex activation increases c-Fos expression in intercalated neurons of the amygdala. Neuroscience *132*, 943–953.

Bissière, S., Humeau, Y., and Lüthi, A. (2003). Dopamine gates LTP induction in lateral amygdala by suppressing feedforward inhibition. Nat. Neurosci. *6*, 587–592.

Busti, D., Geracitano, R., Whittle, N., Dalezios, Y., Mańko, M., Kaufmann, W., Sätzler, K., Singewald, N., Capogna, M., and Ferraguti, F. (2011). Different fear states engage distinct networks within the intercalated cell clusters of the amygdala. J. Neurosci. *31*, 5131–5144.

Cho, J.H., Deisseroth, K., and Bolshakov, V.Y. (2013). Synaptic encoding of fear extinction in mPFC-amygdala circuits. Neuron *80*, 1491–1507.

Corcoran, K.A., and Quirk, G.J. (2007). Activity in prelimbic cortex is necessary for the expression of learned, but not innate, fears. J. Neurosci. *27*, 840–844.

Davis, M., and Whalen, P.J. (2001). The amygdala: vigilance and emotion. Mol. Psychiatry *6*, 13–34.

Delamater, A.R. (2004). Experimental extinction in Pavlovian conditioning: behavioural and neuroscience perspectives. Q. J. Exp. Psychol. B *57*, 97–132.

Duvarci, S., and Pare, D. (2014). Amygdala microcircuits controlling learned fear. Neuron *82*, 966–980.

Ehrlich, I., Humeau, Y., Grenier, F., Ciocchi, S., Herry, C., and Lüthi, A. (2009). Amygdala inhibitory circuits and the control of fear memory. Neuron *62*, 757–771.

Falls, W.A., Miserendino, M.J., and Davis, M. (1992). Extinction of fear-potentiated startle: blockade by infusion of an NMDA antagonist into the amygdala. J. Neurosci. *12*, 854–863.

Geracitano, R., Kaufmann, W.A., Szabo, G., Ferraguti, F., and Capogna, M. (2007). Synaptic heterogeneity between mouse paracapsular intercalated neurons of the amygdala. J. Physiol. *585*, 117–134.

Guarraci, F.A., Frohardt, R.J., Young, S.L., and Kapp, B.S. (1999). A functional role for dopamine transmission in the amygdala during conditioned fear. Ann. N Y Acad. Sci. *877*, 732–736.

Herry, C., Trifilieff, P., Micheau, J., Lüthi, A., and Mons, N. (2006). Extinction of auditory fear conditioning requires MAPK/ERK activation in the basolateral amygdala. Eur. J. Neurosci. *24*, 261–269.

Herry, C., Ciocchi, S., Senn, V., Demmou, L., Müller, C., and Lüthi, A. (2008). Switching on and off fear by distinct neuronal circuits. Nature *454*, 600–606.

Hübner, C., Bosch, D., Gall, A., Lüthi, A., and Ehrlich, I. (2014). Ex vivo dissection of optogenetically activated mPFC and hippocampal inputs to neurons in the basolateral amygdala: implications for fear and emotional memory. Front. Behav. Neurosci. *8*, 64.

Inglis, F.M., and Moghaddam, B. (1999). Dopaminergic innervation of the amygdala is highly responsive to stress. J. Neurochem. *72*, 1088–1094.

Jacobsen, K.X., Höistad, M., Staines, W.A., and Fuxe, K. (2006). The distribution of dopamine D1 receptor and mu-opioid receptor 1 receptor immunoreactivities in the amygdala and interstitial nucleus of the posterior limb of the anterior commissure: relationships to tyrosine hydroxylase and opioid peptide terminal systems. Neuroscience *141*, 2007–2018.

Laurent, V., and Westbrook, R.F. (2008). Distinct contributions of the basolateral amygdala and the medial prefrontal cortex to learning and relearning extinction of context conditioned fear. Learn. Mem. *15*, 657–666.

LeDoux, J.E., Sakaguchi, A., and Reis, D.J. (1984). Subcortical efferent projections of the medial geniculate nucleus mediate emotional responses conditioned to acoustic stimuli. J. Neurosci. *4*, 683–698.

LeDoux, J.E., Farb, C.R., and Milner, T.A. (1991). Ultrastructure and synaptic associations of auditory thalamo-amygdala projections in the rat. Exp. Brain Res. *85*, 577–586.

Likhtik, E., Pelletier, J.G., Paz, R., and Paré, D. (2005). Prefrontal control of the amygdala. J. Neurosci. *25*, 7429–7437.

Likhtik, E., Popa, D., Apergis-Schoute, J., Fidacaro, G.A., and Paré, D. (2008). Amygdala intercalated neurons are required for expression of fear extinction. Nature *454*, 642–645.

Lopez de Armentia, M., and Sah, P. (2004). Firing properties and connectivity of neurons in the rat lateral central nucleus of the amygdala. J. Neurophysiol. *92*, 1285–1294.

Marek, R., Strobel, C., Bredy, T.W., and Sah, P. (2013). The amygdala and medial prefrontal cortex: partners in the fear circuit. J. Physiol. *591*, 2381–2391.

Maren, S. (2001). Neurobiology of Pavlovian fear conditioning. Annu. Rev. Neurosci. *24*, 897–931.

(J) Percentage of cells that demonstrated disynaptic inhibition at −40 mV, either following monosynaptic excitatory inputs (EPSC and IPSC, blue), or disynaptic inhibition alone (di-IPSC, orange). Example traces are depicted next to the graph. The schematic summarizes the possible source of disynaptic inhibition in the ITC clusters.
Error bars indicate mean ± SEM.

Marowsky, A., Yanagawa, Y., Obata, K., and Vogt, K.E. (2005). A specialized subclass of interneurons mediates dopaminergic facilitation of amygdala function. Neuron *48*, 1025–1037.

Mascagni, F., McDonald, A.J., and Coleman, J.R. (1993). Corticoamygdaloid and corticocortical projections of the rat temporal cortex: a Phaseolus vulgaris leucoagglutinin study. Neuroscience *57*, 697–715.

McDonald, A.J. (1982). Neurons of the lateral and basolateral amygdaloid nuclei: a Golgi study in the rat. J. Comp. Neurol. *212*, 293–312.

McDonald, A.J. (1985). Immunohistochemical identification of gamma-aminobutyric acid-containing neurons in the rat basolateral amygdala. Neurosci. Lett. *53*, 203–207.

McDonald, A.J. (1998). Cortical pathways to the mammalian amygdala. Prog. Neurobiol. *55*, 257–332.

Mcdonald, A.J., Mascagni, F., and Guo, L. (1996). Projections of the medial and lateral prefrontal cortices to the amygdala: a Phaseolus vulgaris leucoagglutinin study in the rat. Neuroscience *71*, 55–75.

Milad, M.R., and Quirk, G.J. (2002). Neurons in medial prefrontal cortex signal memory for fear extinction. Nature *420*, 70–74.

Millhouse, O.E. (1986). The intercalated cells of the amygdala. J. Comp. Neurol. *247*, 246–271.

Miserendino, M.J.D., Sananes, C.B., Melia, K.R., and Davis, M. (1990). Blocking of acquisition but not expression of conditioned fear-potentiated startle by NMDA antagonists in the amygdala. Nature *345*, 716–718.

Morozov, A., Sukato, D., and Ito, W. (2011). Selective suppression of plasticity in amygdala inputs from temporal association cortex by the external capsule. J. Neurosci. *31*, 339–345.

Palomares-Castillo, E., Hernández-Pérez, O.R., Pérez-Carrera, D., Crespo-Ramírez, M., Fuxe, K., and Pérez de la Mora, M. (2012). The intercalated paracapsular islands as a module for integration of signals regulating anxiety in the amygdala. Brain Res. *1476*, 211–234.

Pape, H.C., and Pare, D. (2010). Plastic synaptic networks of the amygdala for the acquisition, expression, and extinction of conditioned fear. Physiol. Rev. *90*, 419–463.

Paré, D., and Smith, Y. (1993). The intercalated cell masses project to the central and medial nuclei of the amygdala in cats. Neuroscience *57*, 1077–1090.

Pare, D., and Duvarci, S. (2012). Amygdala microcircuits mediating fear expression and extinction. Curr. Opin. Neurobiol. *22*, 717–723.

Pinard, C.R., Mascagni, F., and McDonald, A.J. (2012). Medial prefrontal cortical innervation of the intercalated nuclear region of the amygdala. Neuroscience *205*, 112–124.

Pinto, A., and Sesack, S.R. (2008). Ultrastructural analysis of prefrontal cortical inputs to the rat amygdala: spatial relationships to presumed dopamine axons and D1 and D2 receptors. Brain Struct. Funct. *213*, 159–175.

Quirk, G.J., Repa, C., and LeDoux, J.E. (1995). Fear conditioning enhances short-latency auditory responses of lateral amygdala neurons: parallel recordings in the freely behaving rat. Neuron *15*, 1029–1039.

Quirk, G.J., Likhtik, E., Pelletier, J.G., and Paré, D. (2003). Stimulation of medial prefrontal cortex decreases the responsiveness of central amygdala output neurons. J. Neurosci. *23*, 8800–8807.

Romanski, L.M., and LeDoux, J.E. (1993). Information cascade from primary auditory cortex to the amygdala: corticocortical and corticoamygdaloid projections of temporal cortex in the rat. Cereb. Cortex *3*, 515–532.

Romanski, L.M., Clugnet, M.C., Bordi, F., and LeDoux, J.E. (1993). Somatosensory and auditory convergence in the lateral nucleus of the amygdala. Behav. Neurosci. *107*, 444–450.

Royer, S., and Paré, D. (2003). Conservation of total synaptic weight through balanced synaptic depression and potentiation. Nature *422*, 518–522.

Royer, S., Martina, M., and Paré, D. (1999). An inhibitory interface gates impulse traffic between the input and output stations of the amygdala. J. Neurosci. *19*, 10575–10583.

Royer, S., Martina, M., and Paré, D. (2000). Polarized synaptic interactions between intercalated neurons of the amygdala. J. Neurophysiol. *83*, 3509–3518.

Sah, P., Faber, E.S., Lopez De Armentia, M., and Power, J. (2003). The amygdaloid complex: anatomy and physiology. Physiol. Rev. *83*, 803–834.

Sierra-Mercado, D., Padilla-Coreano, N., and Quirk, G.J. (2011). Dissociable roles of prelimbic and infralimbic cortices, ventral hippocampus, and basolateral amygdala in the expression and extinction of conditioned fear. Neuropsychopharmacology *36*, 529–538.

Sotres-Bayon, F., Sierra-Mercado, D., Pardilla-Delgado, E., and Quirk, G.J. (2012). Gating of fear in prelimbic cortex by hippocampal and amygdala inputs. Neuron *76*, 804–812.

Spampanato, J., Polepalli, J., and Sah, P. (2011). Interneurons in the basolateral amygdala. Neuropharmacology *60*, 765–773.

Tamamaki, N., Yanagawa, Y., Tomioka, R., Miyazaki, J., Obata, K., and Kaneko, T. (2003). Green fluorescent protein expression and colocalization with calretinin, parvalbumin, and somatostatin in the GAD67-GFP knock-in mouse. J. Comp. Neurol. *467*, 60–79.

Vertes, R.P. (2004). Differential projections of the infralimbic and prelimbic cortex in the rat. Synapse *51*, 32–58.

Vidal-Gonzalez, I., Vidal-Gonzalez, B., Rauch, S.L., and Quirk, G.J. (2006). Microstimulation reveals opposing influences of prelimbic and infralimbic cortex on the expression of conditioned fear. Learn. Mem. *13*, 728–733.

Wolff, S.B., Gründemann, J., Tovote, P., Krabbe, S., Jacobson, G.A., Müller, C., Herry, C., Ehrlich, I., Friedrich, R.W., Letzkus, J.J., and Lüthi, A. (2014). Amygdala interneuron subtypes control fear learning through disinhibition. Nature *509*, 453–458.